



Reaction of formaldehyde over birnessite catalyst: A combined XPS and ToF-SIMS study

S. Selvakumar^a, N. Nuns^a, M. Trentesaux^a, V.S. Batra^b, J.-M. Giraudon^a, J.-F. Lamonier^{a,*}

^a Univ. Lille, CNRS, Centrale Lille, ENSCL, Univ. Artois, UMR 8181 – UCCS – Unité de Catalyse et Chimie du Solide, F-59000 Lille, France

^b The Energy and Resources Institute (TERI), IHC Complex, Lodi Road, New Delhi 110003 India

ARTICLE INFO

Article history:

Received 15 September 2016

Received in revised form 26 April 2017

Accepted 9 May 2017

Available online 10 May 2017

Keywords:

Formaldehyde

Birnessite

Catalytic oxidation

X-Ray photoelectron spectroscopy

Time of flight secondary ion mass spectrometry

ABSTRACT

Birnessite with very high surface area ($>180 \text{ m}^2 \text{ g}^{-1}$) has been prepared by oxidation of $\text{Mn}(\text{NO}_3)_2$ with H_2O_2 in KOH solution. The catalytic performance of this free noble metal based material for the formaldehyde (HCHO) selective conversion into CO_2 is excellent. Therefore this birnessite material has been selected for X-ray photoelectron spectroscopy (XPS) analysis in combination with time-of-flight secondary ion mass spectroscopy (ToF-SIMS) study to understand the mechanistic interaction between adsorbate and adsorbent. Thermo-desorption of formaldehyde saturated birnessite has been conducted under argon atmosphere, using a catalysis cell allowing the monitoring of the birnessite surface modification. XPS study shows (i) the partial oxidation of formaldehyde at room temperature through the formate species formation and manganese species reduction and (ii) the generation of carbonate species with temperature. ToF-SIMS analyses gave more insight in the kind of cations from birnessite interacting with adsorbed molecules: formate ions interact with manganese and potassium ions while carbonate ions interact only with potassium ions. Formate oxidation takes place on Mn ions to give COx(g) species while formate ions readily decompose on K^+ sites at higher temperature.

© 2017 Elsevier B.V. All rights reserved.

1. Introduction

Indoor emission of formaldehyde (HCHO) has been subject of recent consideration from many governments around the world because HCHO impacts adversely the health of people exposed to this pollutant. The catalytic complete oxidation is regarded as the most promising technology to convert this molecule into harmless species (H_2O , CO_2) [1]. Supported noble metal based materials are very efficient for this reaction since formaldehyde can be converted at ambient temperature [2–6]. Among the noble metals tested (Pt, Pd, Rh, Au), platinum is the most active phase [7]. In particular titania supported platinum doped with Na is shown as the most promising catalytic system for the formaldehyde oxidation [5]. However owing to the high price and limited resources of noble metals, a wide application of these catalysts is highly restricted.

Noble metal free catalysts are proposed to potentially replace noble metal compositions [8]. Bulk and supported transition metal oxides were found to be the low-cost promising materials for low-temperature formaldehyde oxidation [9–12]. Sekine et al. [13] found that manganese dioxide (MnO_2) was the most effective trans-

sition metal oxides for the formaldehyde catalytic removal. The nanostructured MnO_2 /cellulose composites showed excellent catalytic performance in HCHO oxidation [14]. The obtained pure manganese oxide structure and morphology in their study greatly influenced the catalytic performance for HCHO oxidation. Testing different one-dimensional tunnel-type manganese oxide, Chen et al. [15] showed that cryptomelane structure presents much higher catalytic activity in HCHO oxidation than pyrolusite and todorokite.

Birnessite-type manganese oxides are also very active for low-temperature oxidation of formaldehyde [16–21]. Birnessite-type manganese oxides are layered structured materials with edge-shared MnO_6 octahedra forming negatively charged layers, and cations and water molecules are located between the manganese oxide layers. The general formula is $A_x(\text{Mn}^{4+},\text{Mn}^{3+})_2\text{O}_4 \cdot y\text{H}_2\text{O}$ where A is H^+ or metal cation (K^+ , Na^+). A very recent research showed that room-temperature oxidation of formaldehyde is possible using layered manganese oxide, i.e. birnessite as active phase [16]. The authors claim that the formaldehyde conversion was related to the water content in the birnessite. Formate and carbonate species were seen as intermediate products. Remarkably surface carbonate poisoning was suppressed in humid air indicating that water likely assists the carbonate transformation into CO_2 . Studying the effects of interlayer cations [20] and manganese

* Corresponding author.

E-mail address: lamonier@univ-lille1.fr (J.-F. Lamonier).

vacancy [22], Wang et al. highlighted the role of potassium ions enhancing the activity of surface oxygen and resulting in the continuous and complete oxidation of HCHO at room temperature.

The synthesis of manganese based materials with novel morphologies and high surface areas have become an attractive research field. Indeed for the formaldehyde removal at very low concentrations, a hybrid system combining selective formaldehyde adsorption followed by its selective destruction through catalytic oxidation can be an attractive alternative to solve the problem of formaldehyde concentrations at indoor level [23]. The birnessite-type manganese oxides can be prepared by redox precipitation, sol-gel, and hydrothermal processes. The most common and the oldest synthesis protocol is based on the oxidation of Mn (II) by bubbling gaseous oxygen O₂ in strongly basic media. The second synthetic route uses the reduction of Mn (VII) with several reducing agents such as Mn (II) [24], H₂O [25,26], sugars [27], organic acids [28] or organic solvents [29]. An original route for birnessite preparation has been proposed by Eren et al. [30] based on the oxidation of Mn(NO₃)₂ with H₂O₂ in KOH solution. However the textural properties of birnessite prepared in this condition is not specified by the authors. In this study we used this synthesis protocol with the objective of reaching a large specific surface area for birnessite material.

Surface characterization of heterogeneous catalysts is usually done over as-made sample with the objectives to study the dispersion and the nature of the phases formed as well as the metal–metal or metal–support interactions. In addition the monitoring of the evolution of various adsorbed surface species on the catalyst with probe molecules can be useful to identify intermediate products using a combination XPS-FTIR [31] or XPS-TDS [32,33]. Moreover ToF-SIMS in combination with XPS has been successfully implemented in order to investigate the mechanism of catalyst deactivation in oxidation of chlorinated volatile organic compound as well as the role of water in the performances of a post-plasma catalytic process [34,35]. XPS analysis allows an easier quantitative approach, while ToF-SIMS analysis gives molecular information with higher surface sensitivity [36].

In this paper, we have investigated the reaction of formaldehyde over K-birnessite surface using a spectroscopic multi-technic approach based on a combined XPS and ToF-SIMS analyses. The paper is devoted to the study of (i) surface composition over K-birnessite after formaldehyde exposure at 25 °C and (ii) surface composition change through the thermo-desorption process. From this original approach a more complete understanding of the surface chemistry of formaldehyde on K-birnessite surface is expected. Indeed there is no study reporting clear evidence of kind of sites involve in the formation and the transformation of intermediates produced at the surface after formaldehyde adsorption.

2. Experimental methods

2.1. Synthesis of material

Manganese based material was prepared at room temperature by oxidation of Mn(NO₃)₂ with H₂O₂ in KOH solution [30]. An aqueous basic solution of H₂O₂ was first prepared as follows: 200 mL of KOH (0.6 mol L⁻¹) was mixed with 200 mL of 3% H₂O₂. This mixture was then added dropwise to 100 mL of Mn(NO₃)₂·xH₂O solution (0.2 mol L⁻¹) at room temperature. After complete precipitation the final reaction mixture was stirred at room temperature for 2 h and kept at the same temperature for 24 h ageing. The final suspension was filtered and washed with distilled water for several times and dried at 100 °C overnight. The above synthesized material was calcined at different temperature (300 °C, 450 °C and 600 °C) for 3 h under air flow.

In the following while the catalytic tests were performed with the three calcined samples, the formaldehyde adsorption and thermo-desorption studies were conducted over the selected birnessite material, i. e. material calcined at 300 °C and labelled KB from here onwards.

2.2. Catalytic activity test

The formaldehyde catalytic oxidation was carried out in a fixed bed continuous flow microreactor (i.d. 10 mm) loaded with 200 mg of catalyst. Gaseous formaldehyde was generated from solid paraformaldehyde through a permeation tube placed in a permeation chamber (Dynacalibrator®, VICI Metronics, Inc.) which was maintained at a constant temperature (100 °C). The reaction mixture containing 120 ppm HCHO, 20 vol.% O₂ was balanced by He (total flow rate = 100 mL min⁻¹). Experiments were conducted by saturating the catalyst with HCHO at 25 °C. Once saturation was complete, the reaction temperature was increased from room temperature to 200 °C using a heating rate of 1 °C min⁻¹ and the data were collected during the heating run. The effluent gas from the reactor containing formaldehyde, oxygen and carbon dioxide was analyzed on-line by a Varian CP 4900 MicroGC chromatograph equipped with a thermal conductivity detector.

2.3. Adsorption of formaldehyde

The adsorption of HCHO on KB was performed at 25 °C by passing the carrier gas (Ar) through the Dynacalibrator® permeation chamber (100 °C). Before the adsorption step, the KB material was pre-treated with argon at 150 °C to remove water and surface impurities. Surface saturation of the material was followed by mass spectrometry (Omnistar, GSD 301-Pfeiffer). The birnessite was then purged at 25 °C with argon until the physisorbed formaldehyde was removed (2 h). The obtained material was labelled as KB-F25.

2.4. Thermo-desorption of formaldehyde saturated birnessite

The formaldehyde saturated birnessite KB-F25 was placed into a catalysis cell connected to a radial chamber (P = 10⁻⁸ mbar) allowing the monitoring of the birnessite surface by successively two surface analysis techniques, X-ray photoelectron spectroscopy (XPS) and time-of-flight secondary ion mass spectroscopy (ToF-SIMS). The thermo-desorption experiments were conducted in argon atmosphere (30 mL min⁻¹) using the catalysis cell, from 25 °C to 200 °C (2 °C min⁻¹). The maximum temperature was maintained for 15 min. Before being introduced into the radial chamber the sample was cooled down to 25 °C and degassed to reduce pressure to 10⁻⁶ mbar. The solid was labelled KB-FX, where X represents the maximum temperature to which the solid was heated before spectroscopic analysis.

2.5. X-Ray photoelectron spectroscopy (XPS)

XPS experiments were performed using an AXIS Ultra DLD Kratos spectrometer equipped with a monochromatized aluminum source (Al K α = 1486.7 eV) and charge compensation gun. Adventitious carbon contamination is commonly used as a charge reference for XPS spectra and all binding energies were referenced by setting the C–C component to a binding energy of 284.5 eV. The XPS photopeaks with multiple components were resolved by a peak-fitting program assuming a mixed Gaussian (70%)/Lorentzian (30%) peak shape using the software supplied by CasaXPS. Semi-quantitative analysis accounted for a linear background subtraction. The evolution of the surface atomic percentage of the birnessite material upon formaldehyde adsorption and heating is given in Table S1.

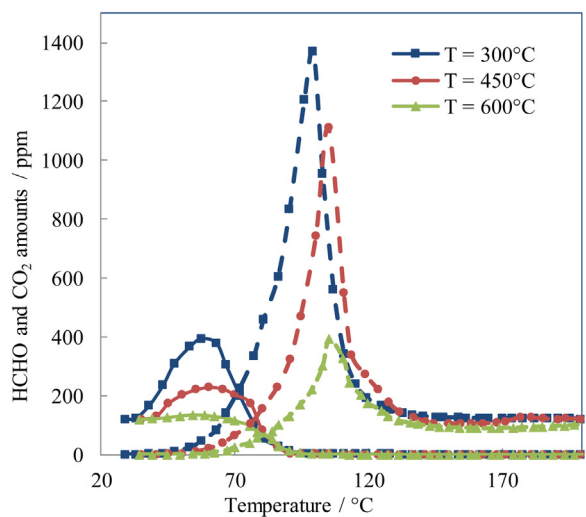


Fig. 1. Evolution of HCHO (straight line) and CO₂ (dotted line) amounts in function of temperature for catalyst previously calcined at different temperatures.

2.6. Time of flight secondary ion mass spectrometry (ToF-SIMS)

ToF-SIMS data were acquired using a ToF-SIMS⁵ spectrometer (ION-TOF GmbH Germany) equipped with a bismuth liquid metal ion gun (LMIG). The samples were bombarded with pulsed Bi³⁺ primary ion beam (25 keV, 0.25 pA) rastered over a 500 μm × 500 μm surface area. With a data acquisition of 100 s, the total fluence does not amount up to 10¹² ions/cm² ensuring static conditions. Charge effects were compensated by means of a 20 eV pulsed electron flood gun. Data were collected over a mass range m/z =0–200 for both positive and negative secondary ions. The fragments were identified by their exact mass, coupled with the appropriate intensities for the expected isotope pattern.

3. Results and discussion

3.1. Characterization and catalytic performance of Mn containing material

Table 1 shows the structural and textural properties obtained for the sample calcined at different temperatures. The birnessite type structure with relative broad diffraction peaks is only observed for sample calcined at 300 °C (Fig. S1). For calcination temperature of 450 °C the α-MnO₂ cryptomelane structure is obtained while at 600 °C a mixture containing the cubic bixbyite structure α-Mn₂O₃ and α-MnO₂ cryptomelane structure is observed (Fig. S1). The average crystallite size (D_c) calculated from the Scherrer equation increases with the calcination temperature in agreement with the decrease of BET surface area (S_{BET}) and total pore volume (V_p) and increase of pore diameter (D_p) (**Table 1**).

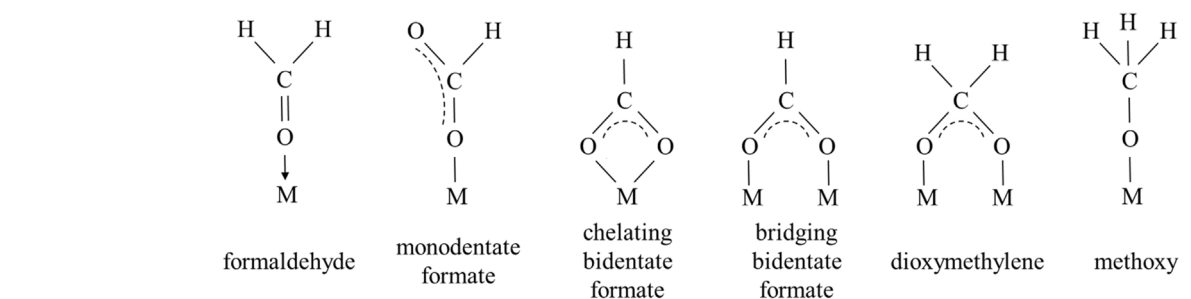


Fig. 2. Possible surface species formed from the formaldehyde interaction with a surface metal site (M).

The BET surface area of the birnessite (184 m² g⁻¹) is much higher than those reported by Tian et al. (145 m² g⁻¹) [17], Chen et al. (70 m² g⁻¹) [18] and Zhou et al. (95 m² g⁻¹) [19] for crystallized K-type birnessite prepared through the reduction of KMnO₄. This result underscores the fact that the oxidation of Mn(NO₃)₂ with H₂O₂ in KOH solution is a suitable process for the preparation of material with very high surface area in comparison with those prepared by reduction of Mn (VII) with other reducing agents.

The different catalysts have been tested in the complete oxidation of formaldehyde. In order to mimic the formaldehyde adsorption phenomena which will be discussed in the next section, experiments were conducted by saturating first the catalyst with HCHO vapor at 25 °C. The evolution of formaldehyde and carbon dioxide amounts is shown (Fig. 1) as a function of temperature in the 25–200 °C range in the presence of the catalyst previously calcined at 300 °C, 450 °C or 600 °C. Irrespective of the calcination temperature, HCHO desorption occurs between 30 °C and 100 °C with a maximum value at around 50 °C. This value is in good agreement with that observed by Quiroz et al. over MnO_x material during HCHO TPD [10]. Carbon dioxide formation also takes place in a single broad peak, between 50 °C and 130 °C, with a maximum at 100 °C for sample calcined at 300 °C and at 110 °C for samples calcined at 450 °C and 600 °C. The quantity of HCHO and CO₂ released is proportional to the specific surface area of the material. The highest SSA birnessite material shows the adsorption of formaldehyde in high quantity at 25 °C. It can be suggested that the formation of surface oxidation products such as formate species [10] which decompose into gaseous CO₂ takes place since the amount of CO₂ is much higher than that expected through the oxidation of 120 ppm of formaldehyde. It is also observed that, irrespective of the calcination temperature, HCHO is completely converted at 100 °C and H₂O and CO₂ are the only products released. Compared with published results, birnessite material synthesized in this study presents comparable catalytic performances for the formaldehyde selective conversion into CO₂ (HCHO conversion of 100% at 100 °C [17]), or even slightly higher (HCHO conversion of 61% at 100 °C) [19].

The preparation of high-specific-surface-area birnessite material can be useful in a two-step adsorption–oxidation process for the formaldehyde removal at very low concentrations [23]. Therefore the material calcined at 300 °C (labelled KB) showing remarkable textural properties has been selected for XPS–ToF-SIMS analyses to obtain information on the mechanism of formaldehyde activation and transformation on the birnessite surface.

3.2. Study of formaldehyde reaction by XPS

3.2.1. Formaldehyde adsorption over birnessite material

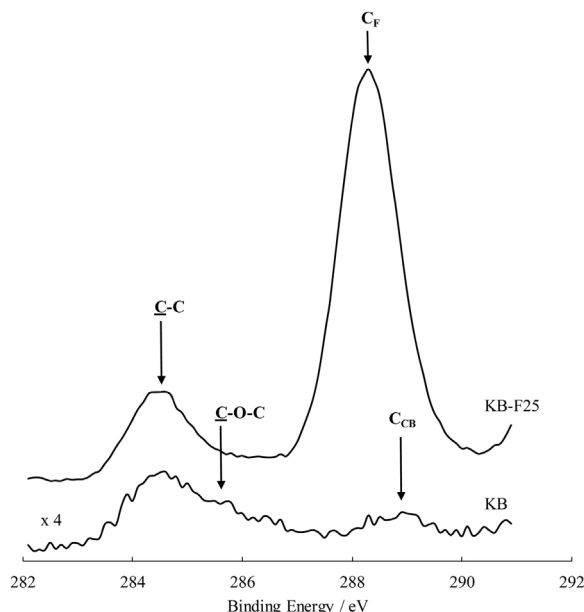
The reactivity of formaldehyde at 25 °C with KB sample was first monitored. Fig. 2 depicts the possible surface species formed from the interaction of HCHO with a surface metal site (M).

Before HCHO adsorption, the as-synthesized birnessite (KB) surface shows three XPS peaks in the C 1 s region at 284.5, 285.5

Table 1

Textural and structural properties of samples calcined at different temperatures.

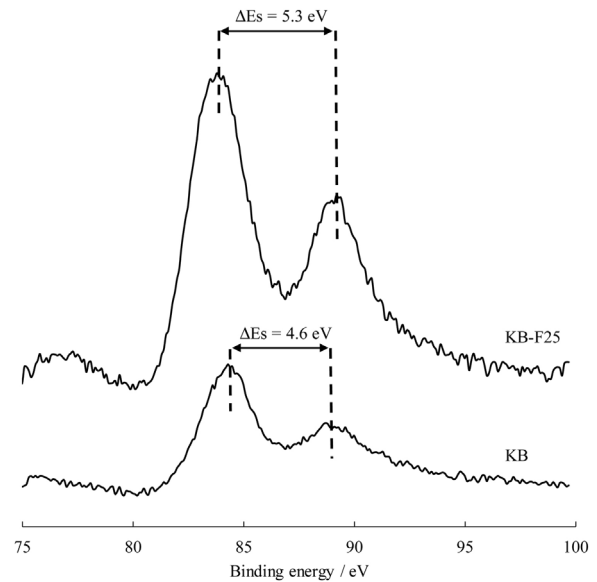
Calcination Temperature/°C	$S_{BET}/m^2 g^{-1}$	$V_p/cm^3 g^{-1}$	D_p/nm	XRD phase	D_c/nm
300	184	0.69	14	$K_x(Mn^{4+},Mn^{3+})_2O_4$	5
450	93	0.62	25	$\alpha-MnO_2$	21
600	42	0.44	44	$\alpha-MnO_2 + \alpha-Mn_2O_3$	28

**Fig. 3.** C 1s XPS signals obtained for KB and KB-F25 samples.

and 289 eV (Fig. 3). The presence of these peaks can be explained by adventitious carbon contamination and can be more precisely attributed to the presence of C–C, C–O–C and O=C=O (carboxylate = C_{CB}) species, respectively [37].

The atomic percentage of carbon at the surface of as-synthesized birnessite corresponds to 3% (Table S1). After HCHO adsorption onto the birnessite surface at 25 °C (KB-F25), this percentage increases significantly (15%) indicating that carbon species are retained on the surface (Table S1). The C 1s core level envelope presents an important contribution at BE of 288.2 eV (C_F). This BE value is lower than that observed for carboxylate species (C_{CB}). The observed binding energy value at 288.2 eV for KB-F25 is close to that observed for adsorbed formaldehyde on rutile TiO_2 (110) surface [32,38]. Based on the report of adsorption of HCHO on rutile TiO_2 (110) surface, it can be suggested that formaldehyde is also associatively adsorbed on the birnessite surface. However C1 s BE should be of the same magnitude for both formate and formaldehyde species, assuming the molecules are bonded end-on through the oxygen atom. Since formation of adsorbed formate species is often proposed as a stable intermediate in the oxidation of formaldehyde [10], the dissociation of formaldehyde into formate ($HCOO^-$) and (H^+) species can also occur. Therefore C_F contribution could arise from both formaldehyde and formate species formation on the birnessite surface.

The partial oxidation of formaldehyde into formate is confirmed by the change in Mn average oxidation state (AOS). XPS spectra of the core levels of Mn 3s are plotted in Fig. 4. Mn3 s photopeak has two multiplet split components due to the coupling of non-ionized 3s electron with 3d valence-band electrons. The two maxima in the binding energy have been evaluated fitting two components in Mn 3s envelope using CasaXPS software. The magnitude of peak splitting (ΔEs) depends on the Mn AOS value, determined from the correlation between the binding energies of the doublet separation

**Fig. 4.** Mn 3s XPS signals obtained for KB and KB-F25 samples.

of Mn 3s (ΔEs) and the AOS, $AOS = 8.956 - 1.13(\Delta Es)$ as proposed by Galakhov et al. [39]. The value of Mn AOS decreases from 3.8 to 3.0 after HCHO adsorption, showing evidence of the reduction of manganese species. This extent of Mn reduction can be readily correlated to the oxidation of the adsorbed formaldehyde into formate species at 25 °C.

Before HCHO adsorption, the as-synthesized birnessite (KB) surface shows one main contribution to O 1s signal at 529 eV which can be unambiguously attributed to lattice oxygen (O_L) (Fig. S2) [40]. Indeed oxygen from metal oxides appears at a significantly lower BE compared to most other oxygen species. After HCHO adsorption (KB-F25), the appearance of second photopoint at higher BE, 531.5 eV is observed along with the photopoint observed for KB sample (Fig. S2). This new photopoint (O_F) can be assigned to O–C and O=C arising from adsorbed formate and formaldehyde species.

K 2p region is composed of a doublet with BE contributions at 292 eV and 294.7 eV which are respectively assigned to K 2p_{3/2} and K 2p_{1/2} of potassium lines (Fig. S3). These values are in good agreement with those reported over K-birnessite material by Thenuwara et al. [41]. No clear modification of the K 2p envelope is seen after HCHO adsorption.

3.2.2. Thermo-desorption of formaldehyde saturated birnessite

Fig. 5 shows the evolution of the C 1s spectrum in the 286.5–290.5 eV range after treatment at different temperatures in argon. Up to 100 °C, the C1 s profile is rather similar with mainly one component (C_F) attributed to formate/formaldehyde species. At 125 °C the maximum of the C1 s signal is shifted to higher BE due to the decrease of the formate/formaldehyde contribution and the joint appearance of a second component (C_{CB}) at higher BE (289.1 eV) attributed to carbonate species [42]. At 175 °C and 200 °C, the C 1s signal includes only the carbonate component at 289.1 eV.

Fig. 6 shows the evolution of the intensity of the two carbon components (C_F and C_{CB}) as a function of temperature together

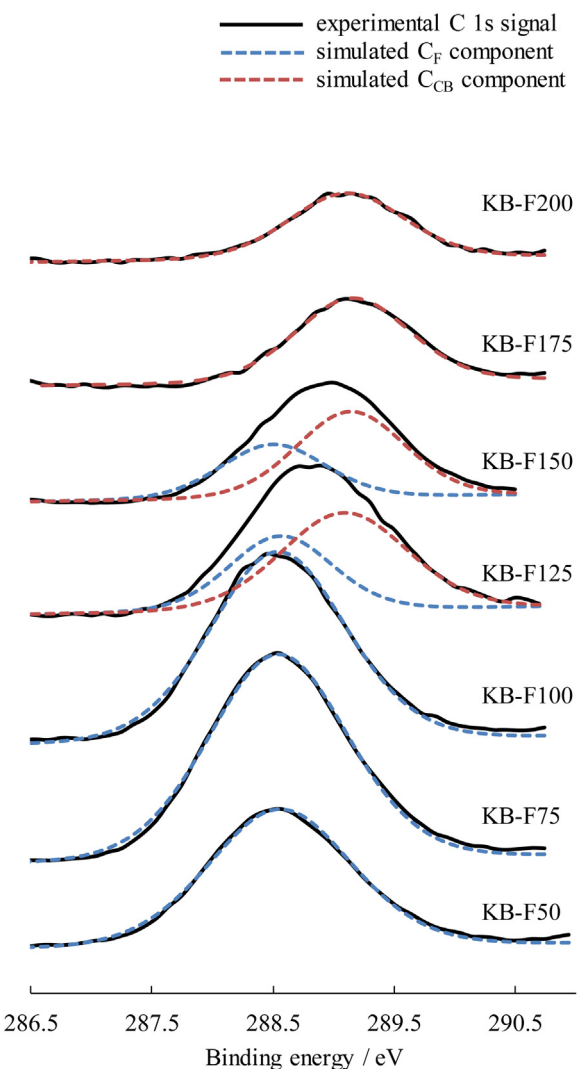


Fig. 5. Evolution of the C 1s XPS signal (straight lines) and components from curve fitting (dotted lines) as a function of temperature treatment from 25 °C to 200 °C.

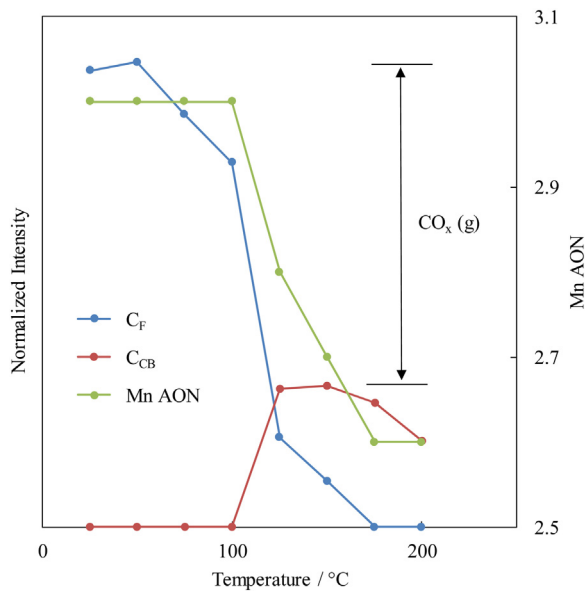


Fig. 6. Evolution of the XPS carbon component intensities (C_F and C_{CB}) and Mn average oxidation number as a function of temperature.

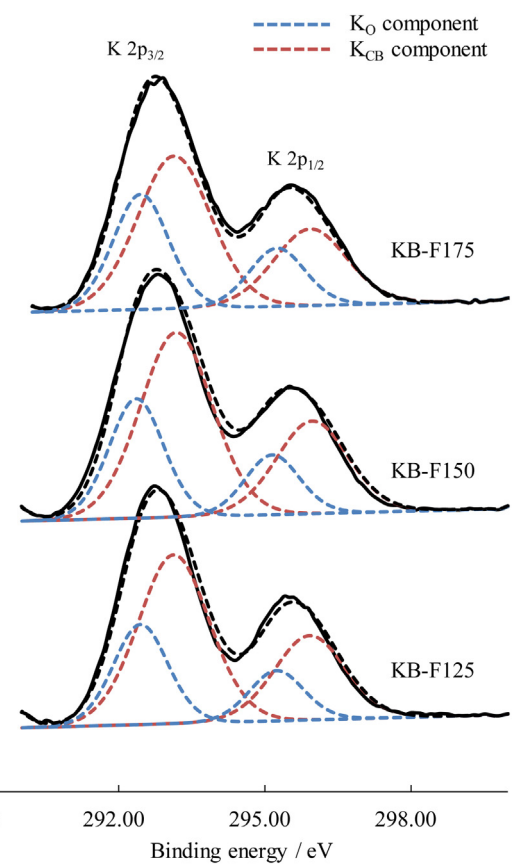


Fig. 7. K 2p XPS signal obtained for KB-F125, KB-F150, KB-F175 samples (straight lines) and components from curve fitting (dotted lines) as a function of temperature treatment from 125 °C to 175 °C.

with the evolution of the average oxidation number of manganese. The XPS peak intensity has been normalized, dividing the carbon component intensity by the Mn 2p photopeak intensity. From 50–100 °C, the C_F component intensity decrease can be explained by the formaldehyde desorption without Mn AOS value change. From 100 °C to 175 °C, the decrease in intensity of C_F component fits well with the decrease in Mn AON. Consequently the formate species are readily oxidized by oxygen species from the birnessite. At 200 °C the birnessite is probably reduced into Mn₃O₄ in accordance with the Mn AON of 2.6. The oxidation process leads to the formation of carbonates species. However in order to explain the incomplete carbon balance (Fig. 6), it can be suggested that there is release of gaseous CO_x species during this process.

Alkali metal carbonates are easily formed on oxide surfaces [42]. Therefore the formation of K₂CO₃ can be proposed owing to the presence of K⁺ ions located between the manganese oxide layers in the birnessite structure. In order to assess this assumption, a curve fitting of the K 2p line into two components has been done for KB-F125, KB-F150 and KB-F175 samples. The results of K 2p spectra curve fitting are shown in Fig. 7 and Table 2. The K 2p_{3/2} BE at 292.4 eV (K_O) is assigned to potassium species residing between the Mn based sheets [43], while the K 2p_{3/2} component at higher BE (293.1–293.3 eV) arises from potassium with carbonate surrounding (K_{CB}). The K_{CB}/C_{CB} atomic ratio is close to 2, in very good agreement with the formation of K₂CO₃ species on the surface detected from 125 °C as seen onwards (Table 2). The formation of carbonates species is not obvious from the O 1s spectrum because of the superposition of the oxygen components coming from the formate and the carboxylate species. Nevertheless for KB-F175 sample, the O 1s component at high BE is shifted to lower

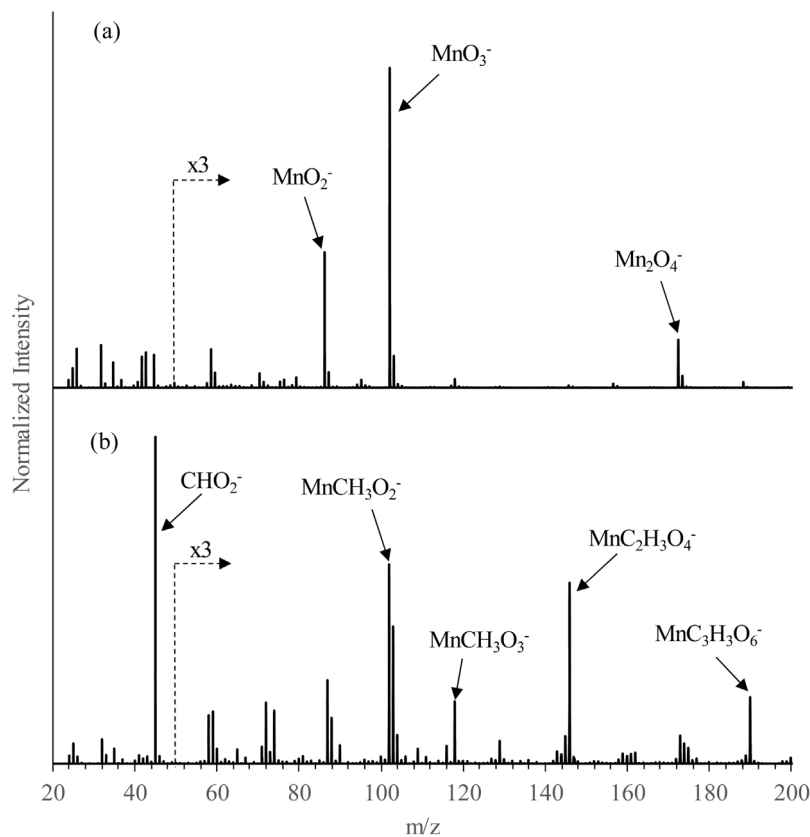


Fig. 8. Negative ToF-SIMS spectra of (a) KB and (b) KB-F25 samples.

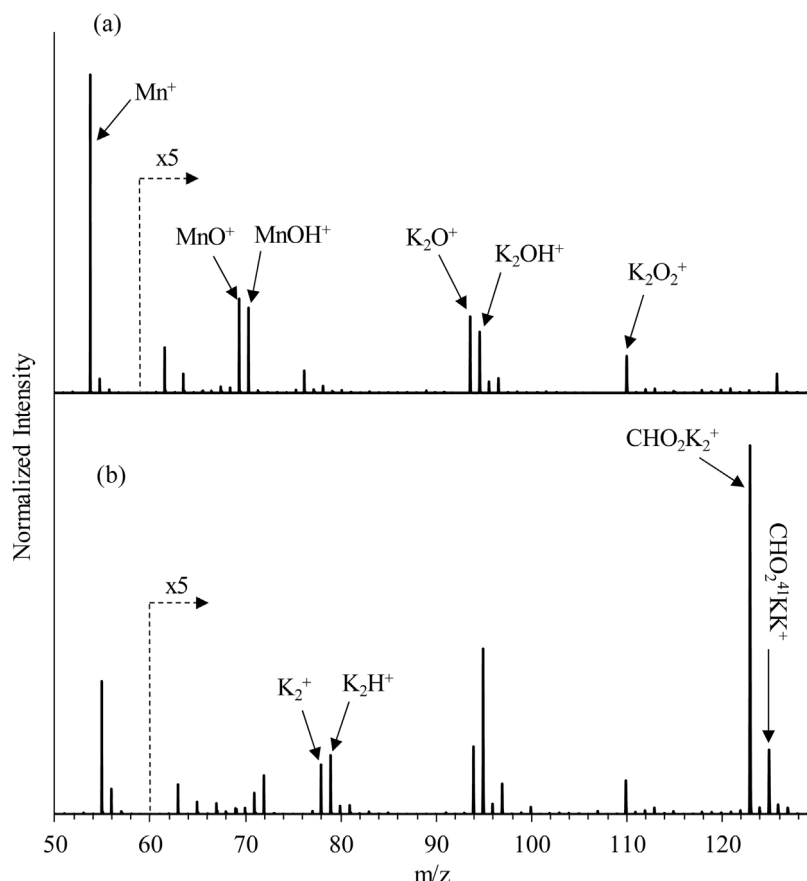


Fig. 9. Positive ToF-SIMS spectra of (a) KB and (b) KB-F25 samples.

Table 2

Binding energy (BE) and Full width at half maximum (FWHM) of the different components issue from the C 1 s and K 2p_{3/2} curve fitting and K_{CB}/C_{CB} atomic ratio as a function of temperature treatment.

sample	C 1s				K 2p _{3/2}				Atomic ratio	
	BE (eV)		FWHM (eV)		BE (eV)		FWHM (eV)			
	C _{CB}	C _F	C _{CB}	C _F	K _{CB}	K _O	K _{CB}	K _O		
KB	289	–	–	–	–	292.3	–	1.4	–	
KB-F25	–	288.3	–	1.3	–	292.3	–	1.4	–	
KB-F50	–	288.3	–	1.3	–	292.3	–	1.4	–	
KB-F75	–	288.5	–	1.3	–	292.4	–	1.5	–	
KB-F100	–	288.5	–	1.3	–	292.4	–	1.5	–	
KB-F125	289.1	288.6	1.2	1.1	293.1	292.4	1.7	1.3	2.0	
KB-F150	289.1	288.5	1.2	1.1	293.2	292.4	1.8	1.3	2.3	
KB-F175	289.1	–	1.1	–	293.1	292.5	1.8	1.4	2.3	
KB-F200	289.1	–	1.1	–	293.3	292.5	1.7	1.5	2.0	

value (-0.5 eV) in comparison with that observed for KB-F samples heated at lower temperature. This could be explained by the disappearance of formate species and the exclusive presence of carbonates at 175°C .

3.3. Study of formaldehyde reaction by ToF-SIMS

3.3.1. Formaldehyde adsorption over birnessite material

ToF-SIMS is able, unlike XPS, to give molecular information about interface through the detection of molecular ions including elements of adsorbent (birnessite) and molecule(s) of adsorbate (formaldehyde/formate). The high mass resolution provided by ToF-SIMS analysis allowed successful discrimination of very close m/z values. For example the mass separation of Mn⁺ ($m/z=54.938$) and OK⁺ ($m/z=54.959$) ions has been possible (Fig. S4). The use of isotopic patterns for the potassium (^{39}K and ^{41}K with respective abundance of 93% and 7%) reinforced the ion assignment. Characteristic secondary ions from birnessite (KB) were assigned and reported in Table S2. Secondary ions relative to potassium are only detected in positive mode while Mn fragment ions are detected in both polarities. Secondary ions containing both K and Mn cations are not detected in the m/z range studied. Figs. 8 and 9 show the negative and positive ToF-SIMS spectra obtained before and after HCHO adsorption on the as-synthesized birnessite surface. For the as-made sample (KB) beyond $m/z=50$ in the negative and positive spectra the following most intense peaks are observed (ion, m/z value): MnO₂[−], 86.9; MnO₃[−], 102.9; Mn₂O₄[−], 173.9, Mn⁺, 54.9; MnO⁺, 70.9; MnOH⁺, 71.9; K₂O⁺, 93.9; K₂OH⁺, 94.9; K₂O₂⁺, 109.9. The ToF-SIMS spectra obtained for KB-F25 sample exhibit additional peaks. In the negative ToF-SIMS spectrum the following characteristic peaks (ion, m/z value) are found: CHO₂[−], 45.0; MnCH₃O₂[−], 101.9; MnCH₃O₃[−], 117.9, MnC₂H₃O₄[−], 145.9; MnC₃H₃O₆[−], 189.9. The most intense peak at 45 m/z is assigned to the presence of formate species, in agreement with XPS results. Interestingly, the ToF-SIMS study shows evidence of formate interaction with Mn, since MnCH_yO_z[−] fragment ions are clearly detected. In the positive spectrum, the following characteristic peaks (ion, m/z value) are found: K₂⁺, 77.9; K₂H⁺, 78.9; K₂CHO₂⁺, 123.9. The important increase in K₂⁺ and K₂H⁺ ions intensity could arise from the presence of K₂CO₃ [44] after formaldehyde adsorption. This interpretation is supported by the detection of other positive ion fragments in the 175–180 m/z range assigned to K₃CO₃⁺ isotopic pattern (Fig. S5).

Furthermore, the presence of K₂CHO₂⁺ fragment ions in the range 120–130 m/z of positive ToF-SIMS spectrum highlights the formate interaction with K. The formation of K₂CHO₂⁺ fragment ions may be the result from the migration of surface formate species from Mn to K site at the birnessite surface.

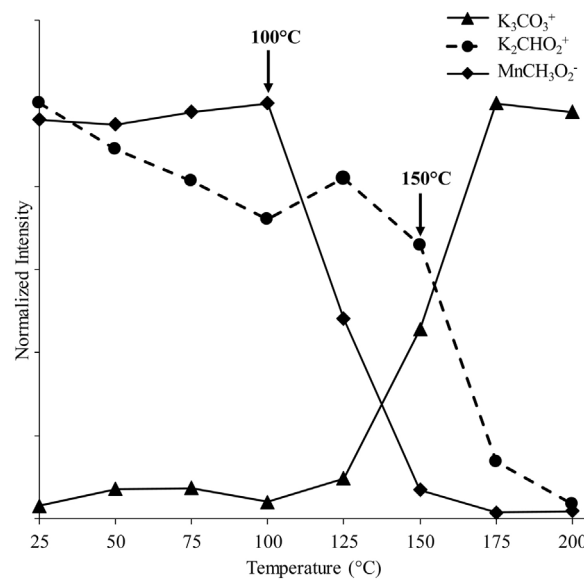


Fig. 10. Evolution of the intensity of MnCH₃O₂[−], K₂CHO₂⁺ and K₃CO₃⁺ fragments with temperature.

3.3.2. Thermo-desorption of formaldehyde saturated birnessite

Fig. 10 shows the evolution of the intensity of MnCH₃O₂[−] ($m/z=101.9$), K₃CO₃⁺ ($m/z=176.9$) and K₂CHO₂⁺ ($m/z=122.9$) fragments with temperature. These secondary ions have the highest m/z among the detected fragments and are representative of one particular species. The intensity of the MnCH₃O₂[−] ion fragment is stable up to 100°C while at 125°C a strong intensity decrease is observed. This result agrees well both with the Mn AON and C_F intensity decreases observed by XPS, the formate species being oxidized on Mn into CO_x(g). While no Mn_xCO_y fragment is detected by ToF-SIMS analysis, a new fragment K₃CO₃⁺ appears starting from 125°C . This result tends to show carbonate formation at the birnessite surface, suggesting that part of gaseous CO_x reacts at the vicinity of potassium species. Moreover a temperature offset related to formate species transformation onto potassium is clearly seen as the intensity of K₂CHO₂⁺ starts to decrease at higher temperature (150°C). In the absence of possible redox mechanism with potassium site, a thermal decomposition of these species could be proposed.

4. Conclusions

In summary, this spectroscopic multi-technic approach allows better insight into the adsorption/oxidation steps of formaldehyde and into the thermo-desorption of intermediate products

in interaction with the K-birnessite. After formaldehyde adsorption/oxidation at 25 °C, formate species were observed at the surface as main products of formaldehyde oxidation. The value of Mn average oxidation number (AON) decreases from 3.8 to 3 after formaldehyde exposure at ambient temperature. While XPS spectroscopy is able to show evidence of formate interaction with Mn species, ToF-SIMS analysis allows the conclusion that formate species are also present on K sites. Different reactivity of formate species has been shown depending on the type of adsorption site. On Mn site, formate species are converted into gaseous CO_x and the Mn AON decreases from 3 to 2.6 according to the transformation of birnessite into Mn₃O₄. The potassium sites are favorable to the carbonate formation and the transformation of formate species in interaction with K takes place at higher temperature through probably a thermal decomposition.

Acknowledgement

The authors thank the Chevreul Institute (FR 2638) for its help in the development of this work. Chevreul Institute is supported by the « Ministère de l'Enseignement Supérieur et de la Recherche », the « Région Nord-Pas de calais » and the « Fonds Européen de Développement des Régions ». Support from Indo-French Centre for the Promotion of Advanced Research (IFCPAR)/Centre Franco-Indien pour la Promotion de La Recherche Avancée (CEFIPRA) is also gratefully acknowledged (Project N°IFC/A/4005-1).

Appendix A. Supplementary data

Supplementary data associated with this article can be found, in the online version, at <http://dx.doi.org/10.1016/j.apcatb.2017.05.029>.

References

- [1] J.Q. Torres, S. Royer, J.-P. Bellat, J.-M. Giraudon, J.-F. Lamonier, Formaldehyde: catalytic oxidation as a promising soft, *ChemSusChem* 6 (2013) 578–592.
- [2] C. Zhang, H. He, K. Tanaka, Catalytic performance and mechanism of a Pt/TiO₂ catalyst for the oxidation of formaldehyde at room temperature, *Appl. Catal. B* 65 (2006) 37–43.
- [3] B.-B. Chen, X.-B. Zhu, M. Crocker, Y. Wang, C. Shi, Complete oxidation of formaldehyde at ambient temperature over γ-Al₂O₃ supported Au catalyst, *Catal. Commun.* 42 (2013) 93–97.
- [4] Q. Xu, W. Lei, X. Li, X. Qi, J. Yu, G. Liu, J. Wang, P. Zhang, Efficient removal of formaldehyde by nanosized gold on well-defined CeO₂ nanorods at room temperature, *Environ. Sci. Technol.* 48 (2014) 9702–9708.
- [5] C. Zhang, F. Liu, Y. Zhai, H. Ariga, N. Yi, Y. Liu, K. Azakura, M. Flytzani-Stephanopoulos, H. He, Alkali-metal-promoted Pt/TiO₂ opens a more efficient pathway to formaldehyde oxidation at ambient temperatures, *Angew. Chem. Int. Ed.* 51 (2012) 1–6.
- [6] Z. Yan, Z. Xu, J. Yu, M. Jaroniec, Enhanced formaldehyde oxidation on CeO₂/AlOOH-supported Pt catalyst at room temperature, *Appl. Catal. B* 199 (2016) 465–468.
- [7] C. Zhang, H. He, A comparative study of TiO₂ supported noble metal catalysts for the oxidation of formaldehyde at room temperature, *Catal. Today* 126 (2007) 345–350.
- [8] S. Royer, D. Duprez, F. Can, X. Courtois, C. Batiot-Dupeyrat, S. Laassiri, H. Alamdari, Perovskites as substitutes of noble metals for heterogeneous catalysis: dream or reality, *Chem. Rev.* 114 (2014) 10292–10368.
- [9] R. Averlant, S. Royer, J.-M. Giraudon, J.-P. Bellat, I. Bezverkhyy, G. Weber, J.-F. Lamonier, Mesoporous silica-confined manganese oxide nanoparticles as highly efficient catalysts for the low-temperature elimination of formaldehyde, *ChemCatChem* 6 (2014) 152–161.
- [10] J. Quiroz, J.-M. Giraudon, A. Gervasini, C. Dujardin, C. Lancelot, M. Trentesaux, J.-F. Lamonier, Total oxidation of formaldehyde over MnO_x CeO₂ catalysts: the effect of acid treatment, *ACS Catal.* 5 (2015) 2260–2269.
- [11] L. Bai, F. Wyrwalski, J.-F. Lamonier, A. Khodakov, E. Monflier, A. Ponchel, Effects of β-cyclodextrin introduction to zirconia-supported cobalt oxide catalysts: from molecule-ion associations to complete oxidation of formaldehyde, *Appl. Catal. B* 138–139 (2013) 381–390.
- [12] P. Liu, H. He, G. Wei, X. Liang, F. Qi, F. Tan, W. Tan, J. Zhu, R. Zhu, Effect of Mn substitution on the promoted formaldehyde oxidation over spinel ferrite: catalyst characterization, performance and reaction mechanism, *Appl. Catal. B* 182 (2016) 476–484.
- [13] Y. Sekine, A. Nishimura, Removal of formaldehyde from indoor air by passive type air-cleaning materials, *Atmos. Environ.* 35 (2001) 2001–2007.
- [14] L. Zhou, J. He, Z. He, Y. Hu, C. Zhang, H. He, Facile in-situ synthesis of manganese dioxide nanosheets on cellulose fibers and their application in oxidative decomposition of formaldehyde, *J. Phys. Chem. C* 115 (2011) 16873–16878.
- [15] T. Chen, H. Dou, X. Li, X. Tang, J. Li, J. Hao, Tunnel structure effect of manganese oxides in complete oxidation of formaldehyde, *Microporous Mesoporous Mater.* 122 (2009) 270–274.
- [16] J. Wang, P. Zhang, J. Li, C. Jiang, R. Yunus, J. Kim, Room-temperature oxidation of formaldehyde by layered manganese oxide: effect of water, *Environ. Sci. Technol.* 49 (2015) 12372–12379.
- [17] H. Tian, J. He, L. Liu, D. Wang, Z. Hao, C. Ma, Highly active manganese oxide catalysts for low-temperature oxidation of formaldehyde, *Microporous Mesoporous Mater.* 151 (2012) 397–402.
- [18] H. Chen, J. He, C. Zhang, H. He, Self-assembly of novel mesoporous manganese oxide nanostructures and their application in oxidative decomposition of formaldehyde, *J. Phys. Chem. C* 111 (2007) 18033–18038.
- [19] L. Zhou, J. Zhang, J. He, Y. Hu, H. Tian, Control over the morphology and structure of manganese oxide by tuning reaction conditions and catalytic performance for formaldehyde oxidation, *Mater. Res. Bull.* 46 (2011) 1714–1722.
- [20] J. Wang, D. Li, P. Li, P. Zhang, Q. Xu, J. Yu, Layered manganese oxides for formaldehyde oxidation at room temperature: the effect of interlayer cations, *RSC Adv.* 5 (2015) 100434–100442.
- [21] J. Li, P. Zhang, J. Wang, M. Wang, Birnessite-type manganese oxide on granular activated carbon for formaldehyde removal at room temperature, *J. Phys. Chem. C* 120 (2016) 24121–24129.
- [22] J. Wang, J. Li, C. Jiang, P. Zhou, P. Zhang, J. Yu, The effect of manganese vacancy in birnessite-type MnO₂ on room-temperature oxidation of formaldehyde in air, *Appl. Catal. B* 204 (2017) 147–155.
- [23] M. Labaki, S. Royer, J.-P. Bellat, I. Bezverkhyy, J.-M. Giraudon, J.-F. Lamonier, Removal of toluene over NaX zeolite exchanged with Cu²⁺, *Catalysts* 5 (2015) 1479–1497.
- [24] J. Luo, Q. Zhang, A. Huang, O. Giraldo, S. Suib, Double-aging method for preparation of stabilized Na-buserite and transformations to todorokites incorporated with various metal, *Inorg. Chem.* 38 (1999) 6106–6113.
- [25] R. Chen, P. Zavalij, M. Whittingham, Hydrothermal synthesis and characterisation of K_xMnO₂·yH₂O, *Chem. Mater.* 8 (1996) 1279–1280.
- [26] S.H. Kim, S.J. Kim, S.M. Oh, Preparation of layered MnO₂ via thermal decomposition of KMnO₄ and its electrochemical characterizations, *Chem. Mater.* 11 (1999) 557–563.
- [27] S. Ching, J.A. Landrigan, M.L. Jorgensen, N. Duan, S.L. Suib, C.L. O'Young, Sol-Gel synthesis of birnessite from KMnO₄ and simple sugars, *Chem. Mater.* 7 (1995) 1604–1606.
- [28] S. Bach, J.P. Pereira-Ramos, N. Baffier, R. Messina, Birnessite manganese dioxide synthesized via a sol-gel process: a new rechargeable cathodic material for lithium batteries, *Electrochim. Acta* 36 (1991) 1595–1603.
- [29] Y. Ma, J. Luo, S. Suib, Syntheses of birnessites using alcohols as reducing reagents: effects of synthesis parameters on the formation of birnessites, *Chem. Mater.* 11 (1999) 1972–1979.
- [30] E. Eren, M. Guney, B. Eren, H. Gumus, Performance of birnessite-type manganese oxide in the thermal-catalytic degradation of polyamide 6, *J. Therm. Anal. Calorim.* 115 (2014) 567–572.
- [31] M.P. Schwartz, R.J. Hamers, Reaction of acetonitrile with the silicon (001) surface: a combined XPS and FTIR study, *Surf. Sci.* 601 (2007) 945–953.
- [32] Q. Yuan, Z. Wu, Y. Jin, F. Xiong, W. Huang, Surface chemistry of formaldehyde on rutile TiO₂(110) surface: photocatalysis vs thermal-catalysis, *J. Phys. Chem. C* 118 (2014) 20420–20428.
- [33] K. Habermehl-Cwirzen, J. Lahtinen, P. Hautojärvi, Methanol on Co (0001): XPS, TDS, WF and LEED results, *Surf. Sci.* 598 (2005) 128–135.
- [34] F. Bertinchamps, C. Poleunis, C. Gregoire, P. Eloy, P. Bertrand, E.M. Gaigneaux, Elucidation of deactivation or resistance mechanisms of CrO_x, VO_x and MnO_x supported phases in the total oxidation of chlorobenzene via ToF-SIMS and XPS analyses, *Surf. Interface Anal.* 40 (2008) 231–238.
- [35] N. Nuns, A. Beaureain, D. Nguyen, A. Vandebroucke, N. De Geyter, R. Morent, C. Leys, J.-M. Giraudon, J.-F. Lamonier, A combined ToF-SIMS and XPS study for the elucidation of the role of water in the performances of a Post-Plasma Process using LaMnO₃ + δ as catalyst in the total oxidation of trichloroethylene, *Appl. Surf. Sci.* 320 (2014) 154–160.
- [36] L.T. Weng, Advances in the surface characterization of heterogeneous catalyst using ToF-SIMS, *Appl. Catal. A* 474 (2014) 203–210.
- [37] L. Islas, J.-C. Ruiz, F. Munoz-Munoz, T. Isoshima, G. Burillo, Surface characterization of poly(vinyl chloride) urinary catheters functionalized with acrylic acid and poly(ethylene glycol) methacrylate using gamma-radiation, *Appl. Surf. Sci.* 384 (2016) 135–142.
- [38] Q. Yuan, Z. Wu, Y. Jin, L. Xu, F. Xiong, Y. Ma, W. Huang, Photocatalytic cross-coupling of methanol and formaldehyde on a rutile TiO₂(110) surface, *J. Am. Chem. Soc.* 135 (2013) 5212–5219.
- [39] V.R. Galakhov, M. Demeter, S. Bartkowski, M. Neumann, N.A. Ovechkina, E.Z. Kurmaev, N.I. Lobachevskaya, Y.M. Mukovskii, J. Mitchell, D.L. Ederer, Mn 3 s exchange splitting in mixed-valence manganites, *Phys. Rev. B: Condens. Matter* 65 (2002) 113102–113105.
- [40] X. Zhang, J. Qin, Y. Xue, P. Yu, B. Zhang, L. Wang, Riping Liu, Effect of aspect ratio and surface defects on the photocatalytic activity of ZnO nanorods, *Sci. Rep.* 4 (2014) (article n(4596)).

[41] A.C. Thenuwara, S.L. Shumlas, N.H. Attanayake, Y.V. Aulin, I.G. McKendry, Q. Qiao, E. Borguet, M.J. Zdilla, D.R. Strongin, Intercalation of cobalt into the interlayer of birnessite improves oxygen evolution catalysis, *ACS Catal.* 6 (2016) 7739–7743.

[42] A.V. Scchukarev, D.V. Korolkov, XPS study of group IA carbonates, *Cent. Eur. J. Chem.* 2 (2004) 347–362.

[43] H. Kim, A. Watthanaphanit, N. Saito, Synthesis of colloidal MnO₂ with a sheet-like structure by one-pot plasma discharge in permanganate aqueous solution, *RSC Adv.* 6 (2016) 2826–2834.

[44] R.L. Mills, Highly stable novel inorganic hybrids, *J. New Mater. Electrochem. Syst.* 6 (2003) 45–54.